

Article

Assessment of Groundwater Vulnerability to Seawater Intrusion Using GALDIT, SITE and SIVI Methods in Laspias River Coastal Aquifer System, NE Greece

Christina Pliaka ^{1,*} , Ioannis Gkiouggis ^{1,*} , Dimitrios Karasogiannidis ¹, Panagiotis Angelidis ¹ ,
Andreas Kallioras ²  and Fotios-Konstantinos Pliakas ^{1,*}

¹ Laboratory of Engineering Geology and Groundwater Research, Department of Civil Engineering, Democritus University of Thrace, 67100 Xanthi, Greece; christinapliaka@gmail.com (C.P.); dimikara92@gmail.com (D.K.); pangelid@civil.duth.gr (P.A.)

² School of Mining & Metallurgical Engineering, National Technical University of Athens, 15773 Athens, Greece; kallioras@metal.ntua.gr

* Correspondence: jgiouggis@civil.duth.gr (I.G.); fpliakas@civil.duth.gr (F.-K.P.)

Abstract: This paper presents the investigation of groundwater vulnerability to seawater intrusion of the aquifer system in the coastal area of Laspias River, NE Greece, for the year 2023, by applying the GALDIT, SITE and SIVI methods, in the context of the groundwater management of the area. The relevant research works include the collection and analysis of data and information regarding the geological and geomorphological environment, as well as the hydrogeological system of the area. The calculation of the GALDIT, SITE and SIVI indices values is described, and the results from the application of the methods are presented, as well as the design of relevant groundwater vulnerability maps of the study area. This paper concludes with findings and proposals useful for the reliable assessment of the hydrogeological regime of the wider study area.

Keywords: coastal aquifer vulnerability; hydrogeological research; groundwater hydrochemical evaluation; GALDIT; SITE; SIVI



Citation: Pliaka, C.; Gkiouggis, I.; Karasogiannidis, D.; Angelidis, P.; Kallioras, A.; Pliakas, F.-K. Assessment of Groundwater Vulnerability to Seawater Intrusion Using GALDIT, SITE and SIVI Methods in Laspias River Coastal Aquifer System, NE Greece. *Water* **2024**, *16*, 1341. <https://doi.org/10.3390/w16101341>

Academic Editor: Chin H Wu

Received: 3 April 2024

Revised: 24 April 2024

Accepted: 30 April 2024

Published: 8 May 2024



Copyright: © 2024 by the authors. Licensee MDPI, Basel, Switzerland. This article is an open access article distributed under the terms and conditions of the Creative Commons Attribution (CC BY) license (<https://creativecommons.org/licenses/by/4.0/>).

1. Introduction

Coastal zones are among the most important areas around the globe as they are among the most populated and invested-in regions [1–3]. Seawater intrusion is among the main threatening factors for the quantity and quality of groundwater resources in coastal aquifers worldwide. A type of popular and easy-to-use approach in the study of seawater intrusion vulnerability assessments is the indexing method [4]. Very little published guidance can be found for rapidly assessing the vulnerability of coastal aquifers to seawater intrusion at regional scales (i.e., aquifer scale), particularly in the case of insufficient long-term data [5–8].

Two well-known indices are called GALDIT and SITE, which would serve as the foundation for the creation of the seawater intrusion vulnerability index (SIVI), a new index designed to address some of these deficiencies [9]. Each of these two indices has benefits and drawbacks.

The vulnerability of the aquifer to seawater intrusion has been calculated using an index called GALDIT, which is based on six parameters: groundwater occurrence, aquifer hydraulic conductivity, height of groundwater level above sea elevation, distance from shore, impact magnitude of the current seawater intrusion and aquifer thickness [10]. For evaluating the possible long-term effects of groundwater use on seawater intrusion, GALDIT has been extensively utilized [8,11–18]. Using its hydrogeological data, the GALDIT indicator model is applied to a region of interest, assigning ratings based on the particular conditions, including seawater intrusion. As a result, locations that are more

vulnerable to seawater intrusion than other places can be defined. It is crucial to note that the GALDIT index is a relative tool and does not eliminate the requirement for more thorough field research [11].

One of the newest indices for assessing groundwater quality impacts was developed by [19]. In order to evaluate the susceptibility of coastal aquifers in Spain to seawater intrusion, they created the SITE index (Surface area affected, Intensity of salinization, Temporality, Evolution over the medium- to long-term). There are certain restrictions on each of the indexes listed. For instance, the SITE index lacks intrinsic qualities, and the GALDIT index ignores the region's dynamic properties. These shortcomings have prompted other researchers to enhance them through the application of fresh methodologies or the fusion of them [9].

The SITE index's goal is to characterize the intrusion process in a form that is simple to calculate and understand [19]. It is based on data that are readily available and easy to obtain. The technique provides numerical and alphabetic findings that enable both qualitative and quantitative differentiation between the water quality statuses of various aquifers. It is based on the concentrations of chloride ions in groundwater at various sites in the aquifer over time.

When compared to other indices, the SITE index has the following benefits [9]: 1. The only necessary data are those for the Cl concentration, which is typically obtained in the majority of monitoring wells. Other water quality metrics, including the HCO_3 ion, which is not measured in some stations, are required for some indices. 2. Simplicity: The concepts and phrasing are simple to use and comprehend. But there are also certain restrictions with the SITE index. While taking into account the region's intensity and dynamics, it ignores the aquifer's inherent qualities and geographic location. Conversely, the GALDIT index considers the aquifer's fundamental traits, but it ignores its dynamic aspects. It also requires some data on water quality, such as HCO_3 , which are not measured in most groundwater monitoring locations [19].

The following benefits have been considered while proposing the SIVI index [9]: (a) easy input data; (b) covering all elements of vulnerability, including intrinsic and dynamic qualities of the region. This allows the index to address the shortcomings of both indices and package them into a new index.

This paper presents the assessment of groundwater vulnerability to seawater intrusion using GALDIT, SITE and SIVI methods in the coastal area of Laspias River, NE Greece, for the year 2023, in the context of the groundwater management of the area. The related research includes the collection and evaluation of data and information about the geological and geomorphological setting, as well as the area's hydrogeological system. The calculation of the GALDIT, SITE and SIVI indices is discussed, and the outcomes of applying the methodologies are shown, as well as the design of relevant groundwater vulnerability maps for the study area. This paper ends with observations and recommendations for a reliable assessment of the hydrogeological regime of the wider study area.

2. Material and Methods

According to the GALDIT method, the variables that determine the extent of groundwater intrusion in a region include [20–23] groundwater occurrence (G), aquifer hydraulic conductivity (A), height of groundwater level above sea level (L), distance from the beach (distance inland perpendicular from shoreline) (D), impact of current seawater intrusion status (I) and aquifer thickness (T). Each parameter has been given a specific weight (1–4) based on how important it is in relation to seawater intrusion. Furthermore, the parameter value is rated with values of 2.5, 5, 7.5 and 10 and categorized into 4 classes (Table 1). A high ranking denotes a high susceptibility to seawater pollution. The following formula estimates the final GALDIT index:

$$GALDIT\ index = \frac{\sum_{i=1}^6 (W_i \cdot R_i)}{\sum_{i=1}^6 W_i} \quad (1)$$

where R and W are the rating and the weight, respectively. The final GALDIT index vulnerability is classified into high (>7.5), moderate (5–7.5) and low (<5). The high GALDIT index vulnerability illustrates the high vulnerability of the study area.

Table 1. Rating of GALDIT parameters.

Parameter	Weight	Classification	Rating
Groundwater occurrence (G)	1	Confined aquifer	10
		Unconfined aquifer	7.5
		Leaky confined aquifer	5
		Bounded aquifer	2.5
Aquifer hydraulic conductivity (A) (m/d)	3	High	>40
		Medium	40–10
		Low	10–5
		Very low	<5
Height of groundwater level above sea level (L) (m)	4	High	<1.0
		Medium	1.0–1.5
		Low	1.5–2.0
		Very low	>2.0
Distance from the shore (D) (m)	4	High	<2500
		Medium	2500–5000
		Low	5000–7500
		Very low	>7500
Impact of existing status of seawater intrusion (I)	1	High	>2
		Medium	1.5–2.0
		Low	1.0–1.5
		Very low	<1
Thickness of the aquifer (T) (m)	2	High	>10
		Medium	7.5–10
		Low	5–7.5
		Very low	<5

The acronym SITE comes from the following parameters [11]: S: surface area of groundwater affected by salinization, I: intensity of the intrusion, T: temporality or seasonality, E: evolution of seawater intrusion.

In comparison to other seawater intrusion indices, the SIVI index is more broadly applicable because it takes into account the most crucial factors affecting seawater intrusion vulnerability, as proposed by [9]. These factors include (1) the size of the affected area, (2) the intensity of the intrusion, (3) its seasonality, (4) its geographical situation and (5) intrinsic features of the region. The SIVI index's geographically independent applied parameters allow it to be utilized in any coastal aquifer.

The SITE value and SIVI index are calculated by Equations (10) and (11), respectively, as presented in Table 2.

The study area is located in the southern coastal part of Xanthi Prefecture in the eastern Delta of Nestos River, NE Greece (Figure 1). The area is characterized mainly by low relief with small plains and small hilly outcrops in the north part of the study area. The western lands are irrigated by the Laspias River and its interconnected ditches, while the river is the final recipient of the surface water from the hydrographic network and the residual irrigation water from the irrigation network in the study area, as well as the effluent from the Wastewater Treatment Plant of Xanthi Municipality [24].

Table 2. Parameters and equations for calculating SITE index και SIVI index values ([9,19], modified).

Parameter	Equation	Explanation
Surface area of groundwater affected by salinization (S)	$S = \frac{S_a}{S_i}$ (2)	S_i : the total aquifer surface S_a : the surface that exceeds the amount of chloride ion concentration from the reference value V_r
Intensity of the intrusion (I)	$I = \frac{\sum S_{i(>V_r)} Cl_{i(>V_r)}}{S_a}$ (3)	S_i : the surface area (km^2) between the isochloride lines (with a value greater than or equal to V_r) Cl_i : the mean chlorine concentration between two isochloride lines
Temporality or seasonality (T)	$T_0 = \frac{\frac{1}{n} \sum_{x=1}^n f(x) - \bar{f}}{\bar{f}}$ (4)	$f(x)$: the mean chloride concentration for a particular year
	$T = 1.25 \times T_0$ (5)	\bar{f} : the mean of the whole series
Evolution of seawater intrusion (E)	$E = \frac{\overline{Cl_n}}{\overline{Cl_{n-1}}}$ (6)	Cl_n και Cl_{n-1} : the average chloride concentration in the current and preceding situation, respectively
Aquifer type (A)	Unconfined, leaky, confined aquifer	
Hydraulic conductivity (C)	$C = \frac{S_b}{S_i}$ (7)	S_b : the surface that exceeds the amount of hydraulic conductivity from the reference value
Height of groundwater level above sea elevation (H)	$H = \frac{S_c}{S_i}$ (8)	S_c : the surface that the height of groundwater level above sea elevation is less than the reference value
Distance from shoreline (D)	$D = \frac{S_d}{S_i}$ (9)	S_d : the surface that exceeds the amount of distance from shore from the reference value
SITE value	$SITE = \frac{3S + 3(S/4)I + T + E}{30}$ (10)	
SIVI index	$SIVI\ index = \frac{\sum_{i=1}^n P_{avi}}{28}$ (11)	P_{avi} : the i th parameter assigned value

The study area is mainly covered by clay, sandy clay, sand and, in some cases, pebbles [25]. Nearly all the study area is used for agricultural activities, with the main crops being maize, cereals, cotton and sunflower [24].

The existence of the seawater intrusion phenomenon in the unconfined aquifer system is demonstrated and confirmed by relevant hydrogeological analyses of the hydrochemical conditions in the study area. Groundwater overpumping is linked to a qualitative degradation of groundwater primarily caused by human activity [25].

Figure 2 shows the annual rainfall values at the Xanthi meteorological station for the period 2009–2023. A relatively constant value variation is observed for the period 2012–2015, as well as low values in the years 2011, 2016, 2017, 2020 and 2022, with a remarkably low value in 2011 and 2022 and an increasing trend in the years 2018 and 2019, as well as a significant downward trend in the 2019–2023 period (meteorological data from <http://meteosearch.meteo.gr> (accessed on 1 March 2024)).

Figure 3 shows the average annual temperature values at the meteorological station of Xanthi for the period of operation (2009–2023) showing an increasing trend, approximately of the order of $0.8\text{ }^{\circ}\text{C}$, specifically from $15.6\text{ }^{\circ}\text{C}$ to $16.4\text{ }^{\circ}\text{C}$, except for the drop to $15.7\text{ }^{\circ}\text{C}$ from $14.6\text{ }^{\circ}\text{C}$ in 2021 and $16.4\text{ }^{\circ}\text{C}$ from $15.5\text{ }^{\circ}\text{C}$ in 2021.

Within the larger region's Quaternary coastal and alluvial deposits, two hydrogeological systems are identified in the study area [26]. The first hydrogeological system consists of approximately 30 m thick phreatic to semi-confined aquifers. This hydrogeological system gets most of its water from precipitation and from nearby small streams and canals. Alternate confined aquifers with a thickness of approximately 200 m make up the second deeper hydrogeological system of the study area. The recharge of the second system comes from lateral groundwater inflows from the nearby hydrogeological basin of Vistonida Lake [25] and Nestos River infiltration through old, buried riverbeds (Figure 1).

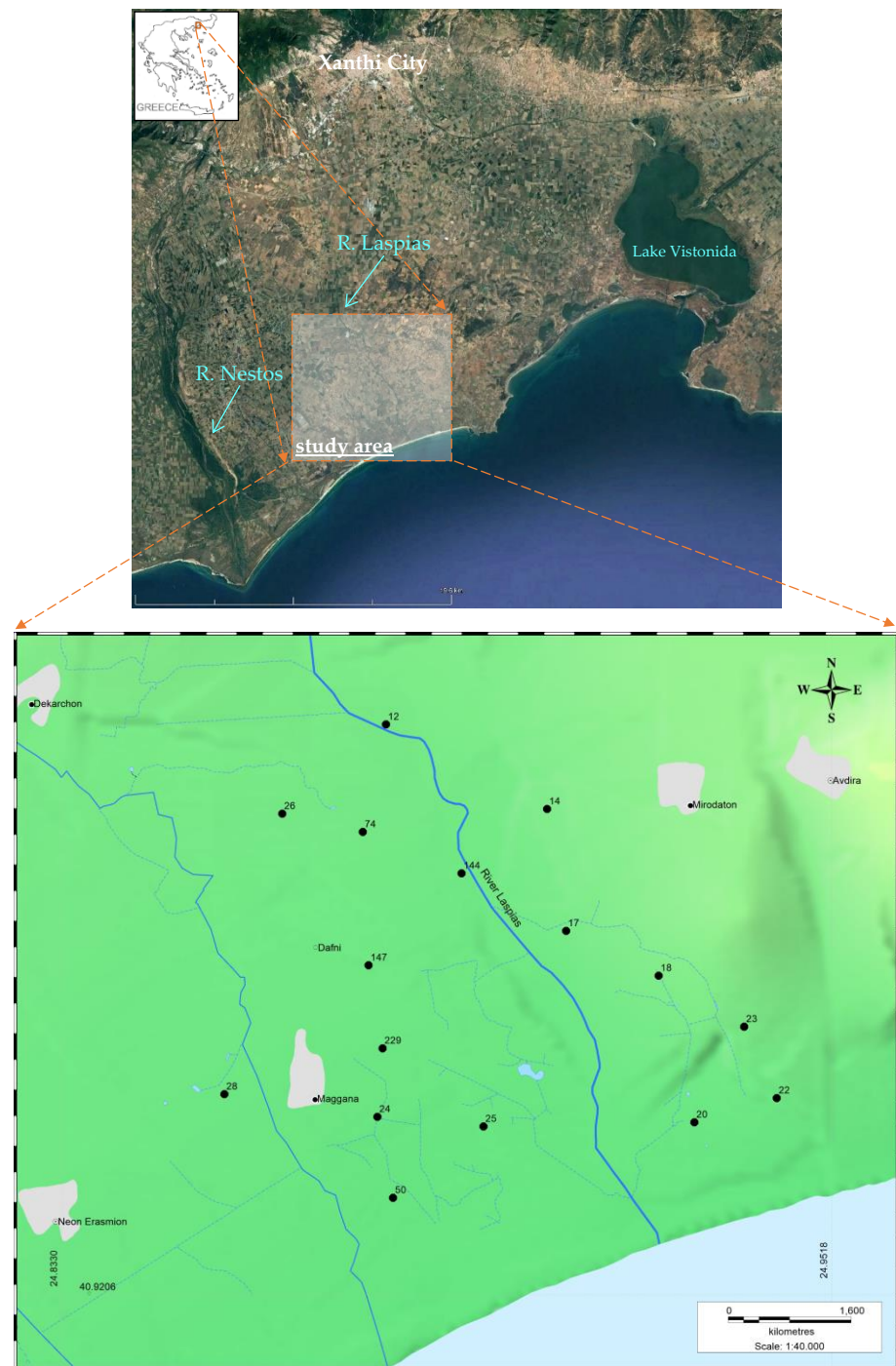


Figure 1. Study area and network of monitoring groundwater wells.

The groundwater level fluctuations were monitored in the study area during the periods April and October 2023, and piezometric maps of the groundwater system of the study area were designed for the studied aquifer (Figure 4), which is recharged mainly from the N-NE part of the study area and from old riverbeds at the SW part of the study area.

The estimation of the groundwater hydraulic parameters after analyzing relevant pumping test data in the broader study area is derived in values for the following [26]: (1) transmissivity (T), ranging from 4.0×10^{-4} to 1.1×10^{-2} m²/s, (2) storage coefficient (S), varying from 10^{-3} to even lower by positions, characterizing the aquifer of the study area as mainly unconfined to semi-confined towards the eastern boundary of the study area. The major groundwater flow direction (Figure 4) is from northwest to south.

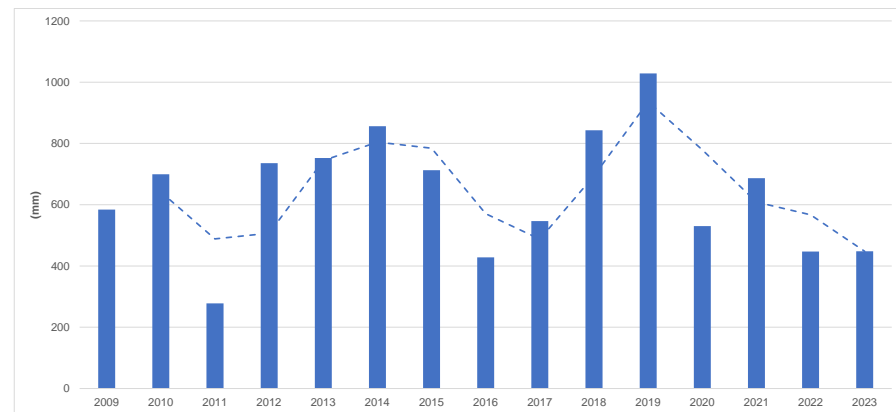


Figure 2. Annual rainfall values (mm) at the Xanthi meteorological station for the period 2009–2023 and moving average of 2 periods (dashed line).

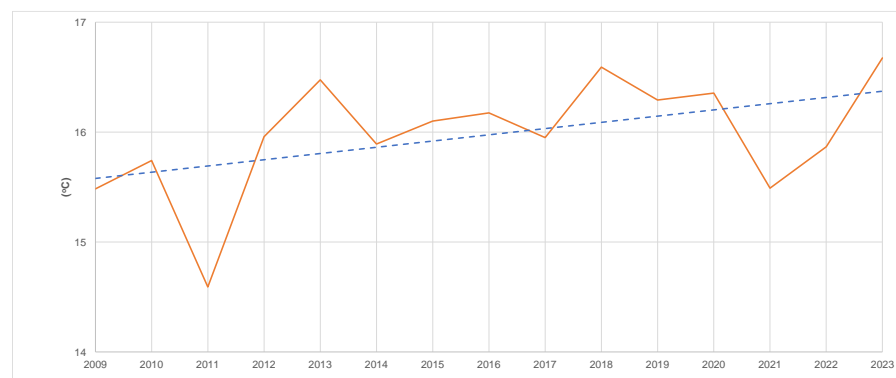


Figure 3. Average annual temperature (°C) values at the Xanthi meteorological station for the period 2009–2023.

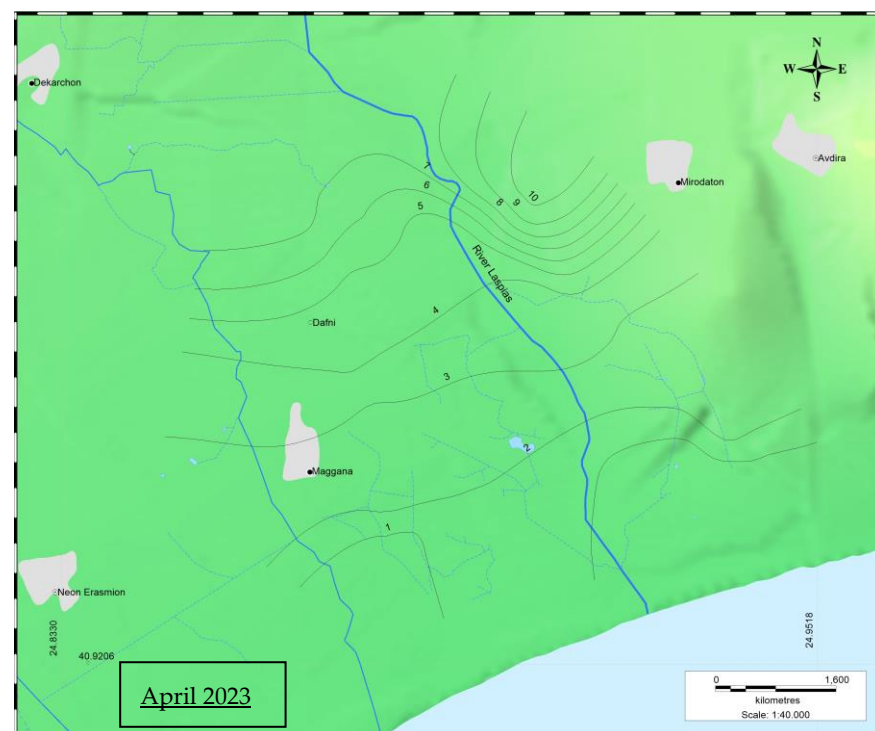


Figure 4. Cont.

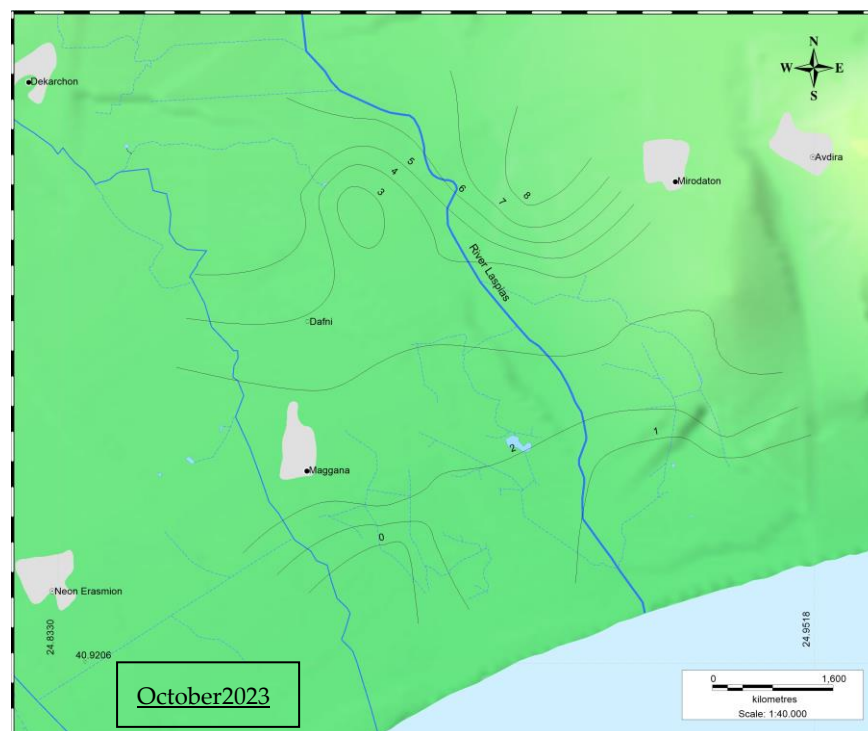


Figure 4. Piezometric maps of the unconfined aquifer of the study area (**upper:** April 2023, **lower:** October 2023).

To monitor the groundwater quality of the study area, a network of 10 sampling wells was selected in such a way to correspond to the under-investigation aquifer and to cover the area as well as possible. The research period included the pumping period of July 2023, where chemical analyses were carried out in the Laboratory of Engineering Geology and Groundwater Research of the Department of Civil Engineering of the Democritus University of Thrace, Greece. The examined parameters were as follows: Ca^{2+} , Mg^{2+} , Na^+ , K^+ , HCO_3^- , Cl^- , SO_4^{2-} , NO_3^- , NO_2^- , NH_4^+ , PO_4^{3-} , SiO_2 , Fe^{2+} , Mn^{2+} , hardness (permanent, non-permanent, total), pH, electrical conductivity (EC).

In Table 3, the statistical analysis of some of the major chemical constituents from groundwater samples (July 2023) is presented (maximum drinking water levels are mentioned, Ca^{2+} : 100 mg/L, Mg^{2+} : 50 mg/L, SO_4^{2-} : 250 mg/L, HCO_3^- : 500 mg/L, PO_4^{2-} : 0.50 mg/L, NO_3^- : 50 mg/L, NO_2^- : 0.5 mg/L, NH_4 : 0.5 mg/L, Cl^- : 250 mg/L, K^+ : 12 mg/L, Na^+ : 200 mg/L, Fe^{2+} : 0.25 mg/L, Mn^{2+} : >0.10 mg/L, EC: 2500 $\mu\text{S}/\text{cm}$, [27]).

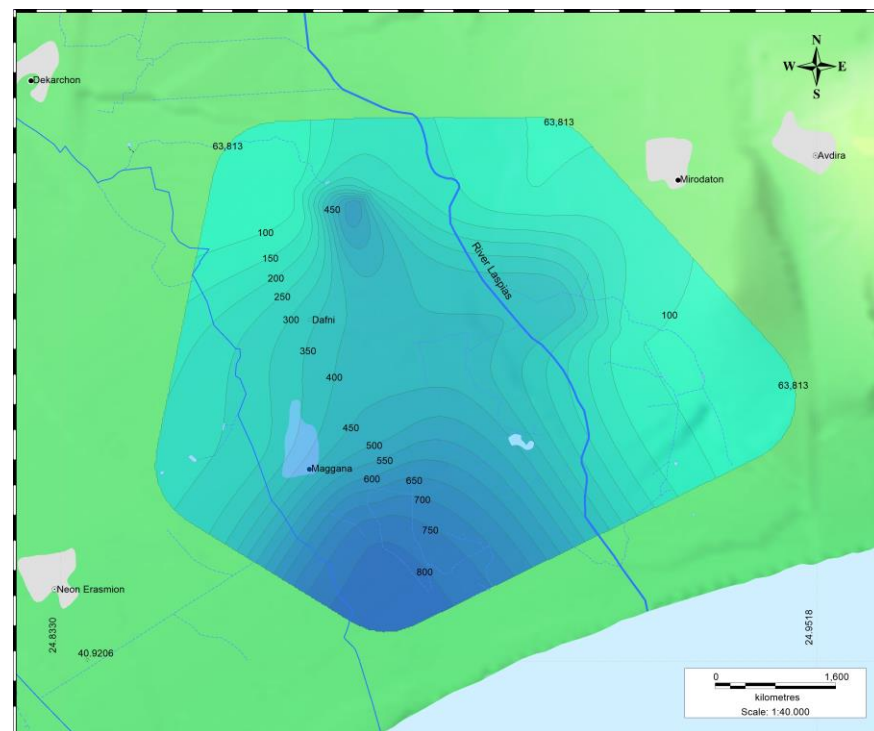
The values of electrical conductivity EC and chlorides Cl^- of the samples range from 652.00 $\mu\text{S}/\text{cm}$ to 3770.00 $\mu\text{S}/\text{cm}$ and from 63.83 mg/L to 815.58 mg/L, respectively (Table 3, Figures 5 and 6). The highest values are observed in the southern coastal part of the study area, where seawater intrusion has been confirmed from previous relevant hydrogeological research in the area [24–26]. Also, some lower values appear and are locally limited in the northern part where a possible influence from the upstream restricted geothermal field outside the main study area has been noticed by [24].

The concentration values of nitrate (NO_3^-) range from 0.00 mg/L to 62.40 mg/L, with four (4) of the ten (10) samples being out of the acceptable limits (allowable: 50 mg/L).

Regarding the suitability of the water samples analyzed for irrigation, based on TDS (Total Dissolved Solids), SAR (Sodium Adsorption Ratio), the concentrations of sodium (Na), chlorine (Cl^-), bicarbonate ion (HCO_3^-), the value criteria %E.sp (%Na, alkalizing degree) and conductivity EC, the results according to ratings and rankings by [28–30], generally all samples were identified as problematic.

Table 3. Statistical analysis of some of the major chemical constituents from groundwater samples (July 2023).

	Min	Max	Aver	SD
Ca ²⁺ (mg/L)	48.10	200.40	115.11	53.66
Mg ²⁺ (mg/L)	9.72	72.90	35.31	21.08
SO ₄ ^{2−} (mg/L)	64.00	300.00	176.10	92.78
HCO ₃ [−] (mg/L)	131.15	895.48	421.27	217.12
PO ₄ ^{2−} (mg/L)	0.13	3.88	1.49	1.14
NO ₃ [−] (mg/L)	0.00	62.40	31.33	24.30
Cl [−] (mg/L)	63.83	815.58	326.41	251.69
EC (μS/cm)	652.00	3770.00	1944.80	966.39
pH	6.72	7.86	7.27	0.30
K ⁺ (mg/L)	2.50	34.30	12.41	9.33
Na ⁺ (mg/L)	105.00	500.00	258.00	148.70
Fe ²⁺ (mg/L)	0.00	0.96	0.16	0.30
Mn ²⁺ (mg/L)	0.50	4.90	1.55	1.28
Na ⁺ /Cl [−]	0.75	2.54	1.58	0.64
SO ₄ ^{2−} /Cl [−]	0.18	1.38	0.60	0.42
(Ca ²⁺ +Mg ²⁺)/(Na ⁺ +K ⁺)	0.18	1.50	0.89	0.40

**Figure 5.** Chloride ion (Cl[−]) distribution map of the unconfined aquifer of the study area (mg/L) (July 2023).

The SAR (Sodium Adsorption Ratio) values range from 1.90 to 15.38. The parts of the study area that face increased serious problems (SAR value > 6) regarding quality degradation due to increased SAR value, are the south-southwest and the central to eastern part (Figure 7). In these parts, where the SAR value exceeds 6, there seems to be a risk of toxicity for the existing crops.

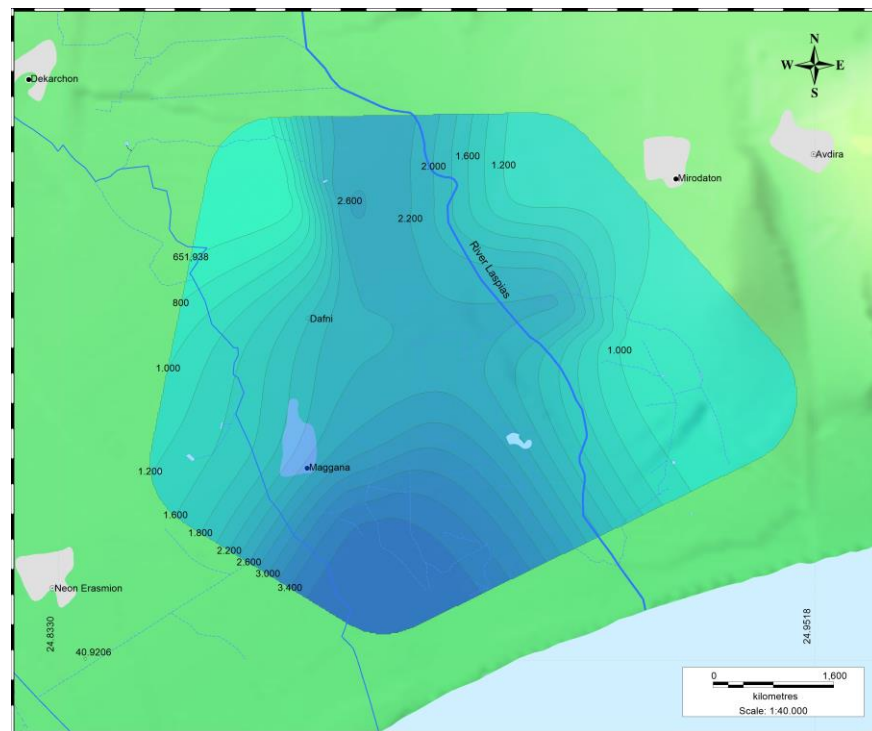


Figure 6. Electrical conductivity distribution map ($\mu\text{S}/\text{cm}$) of the unconfined aquifer of the study area (July 2023).

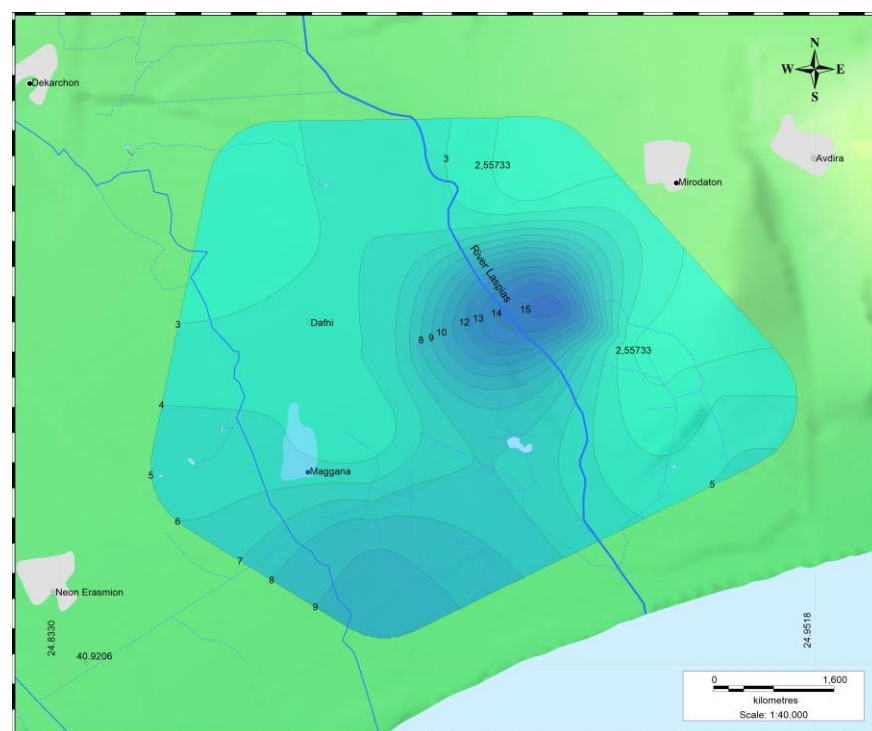


Figure 7. SAR (Sodium Adsorption Ratio) values distribution map of the unconfined aquifer of the study area (July 2023).

The use of the ratio $\text{Cl}/(\text{CO}_3 + \text{HCO}_3)$ in meq/L , which is also referred to as the Revelle coefficient, was proposed as a criterion for seawater penetration [31] in order to prevent an incorrect diagnosis of seawater intrusion caused by a temporary increase in TDS. The range of Revelle values from 1 to 10 indicates moderate to severe pollution caused by

seawater intrusion, while values greater than 10 may be considered evidence of serious pollution [27]. The study area's groundwater is found to be "good" to "slightly polluted" by seawater intrusion, according to Revelle values (min value: 0.40, max value: 3.57, average value: 1.34) (Figure 8).

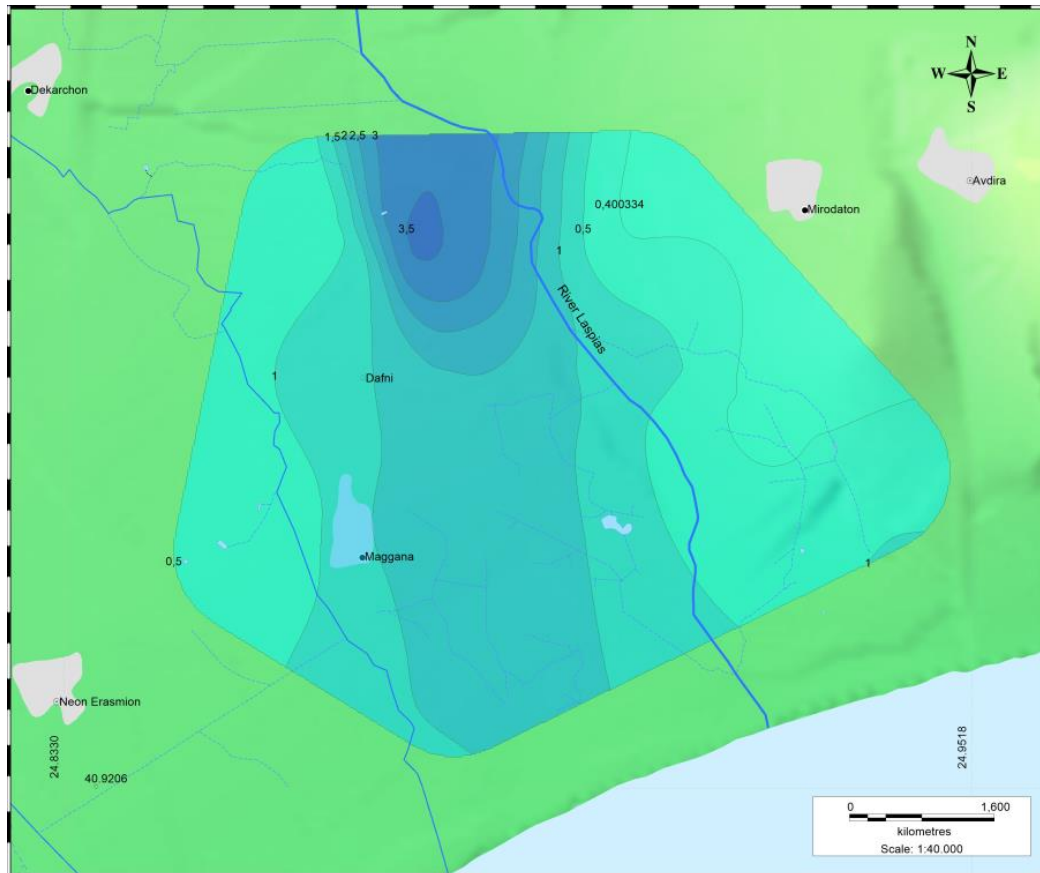


Figure 8. Revelle values distribution map of the unconfined aquifer of the study area (July 2023).

Subsequently, the ionic ratios Na^+/Cl^- , $\text{SO}_4^{2-}/\text{Cl}^-$ and $(\text{Ca}^{2+}+\text{Mg}^{2+})/(\text{Na}^++\text{K}^+)$ were calculated, and relative hydrochemical maps were designed (Figures 9–11). The relevant concluding remarks are summarized in the following:

- The Na^+/Cl^- ratio is related to groundwater salinization and seawater intrusion or to the existence of residual saline deposits within the aquifer [32]. The north part and the south coastal part of the area are considered problematic, as groundwater has undergone salinization ($\text{Na}^+/\text{Cl}^- < 0.876 \pm 10\%$).
- The $\text{SO}_4^{2-}/\text{Cl}^-$ ratio demonstrates the evolution of the salinity of aquifers and is also used to investigate the hydrochemical conditions of coastal aquifers [32]. In the north and the S-SW coastal section of the aquifer, it appears that groundwater is chlorinated or of seawater origin ($\text{SO}_4^{2-}/\text{Cl}^- = 0.1\text{--}0.2$).
- The ionic ratio $(\text{Ca}^{2+}+\text{Mg}^{2+})/(\text{Na}^++\text{K}^+)$ is related to groundwater recharge and gives information about the areas where the groundwater is recharged [27]. Noticeable inflows from the west and the north are detected ($(\text{Ca}^{2+}+\text{Mg}^{2+})/(\text{Na}^++\text{K}^+) > 1$), a finding which is also confirmed in the piezometric maps in Figure 4. Sections of low recharge are located in the S and SW coastal sections.

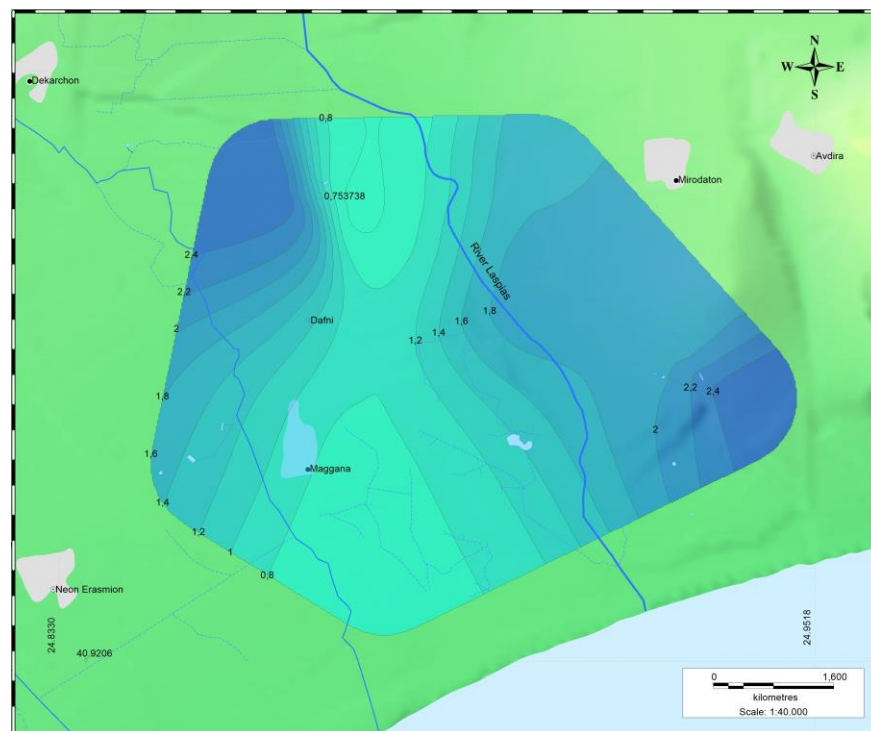


Figure 9. Na^+/Cl^- ratio distribution maps of the unconfined aquifer of the study area (July 2023).

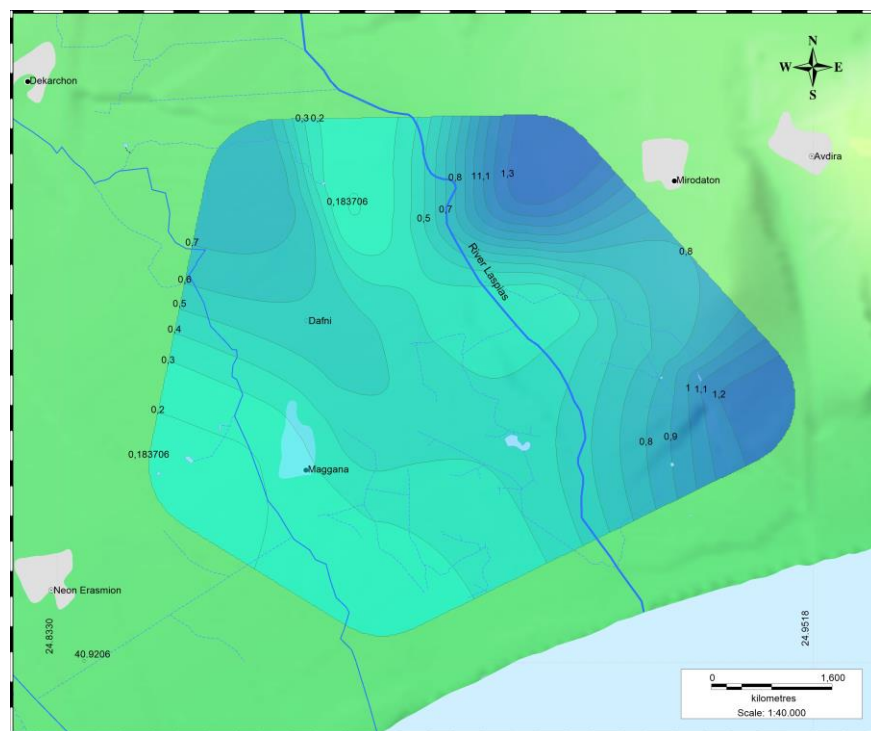


Figure 10. $\text{SO}_4^{2-}/\text{Cl}^-$ ratio distribution maps of the unconfined aquifer of the study area (July 2023).

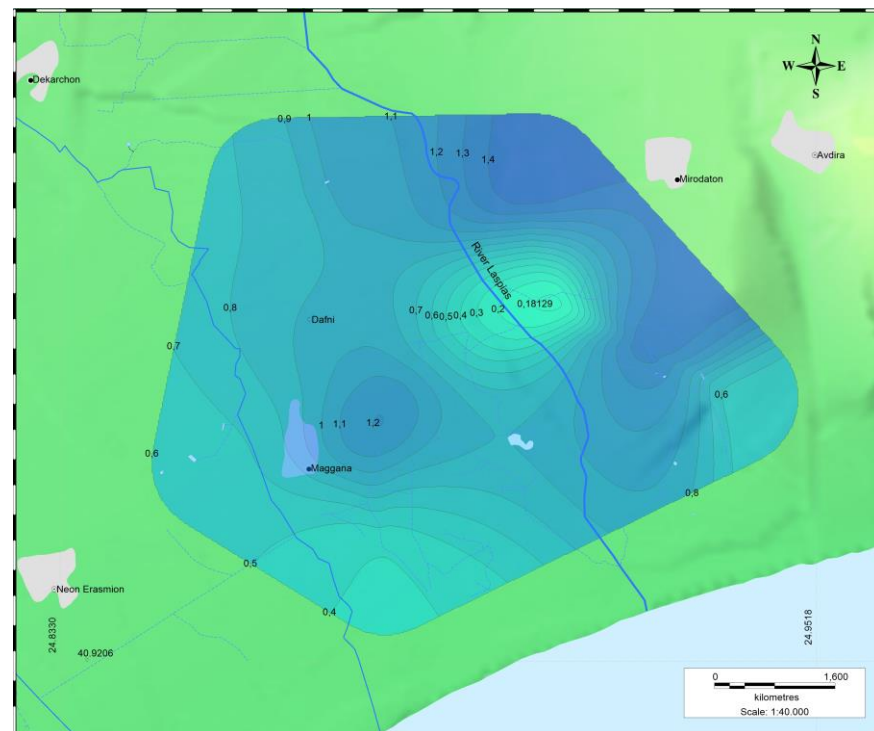


Figure 11. $(\text{Ca}^{2+}+\text{Mg}^{2+})/(\text{K}^{+}+\text{Na}^{+})$ ratio distribution map of the unconfined aquifer of the study area (July 2023).

Finally, as far as the Piper diagram in Figure 12 is concerned, all groundwater samples points are located at the upper part of the rhombic diagram.

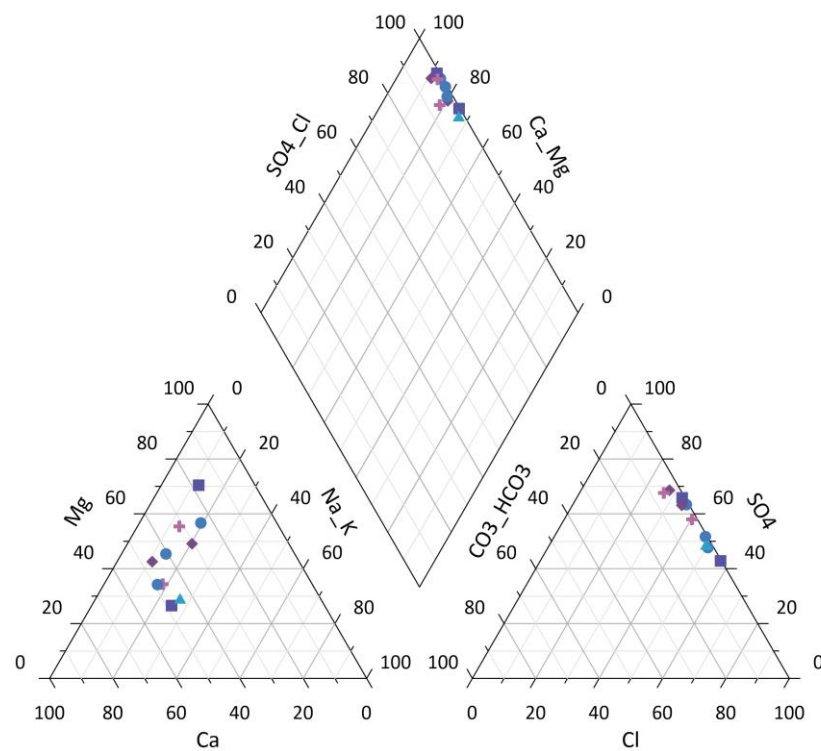


Figure 12. Trilinear Piper diagram for all the wells of the study area (July 2023).

3. Results and Discussion

In the following, the calculation of the GALDIT, SIVI and SITE vulnerability indices is described, both as a general assessment and characterization of the vulnerability of the groundwater system of the research area for April and October 2023, as well as a spatial distribution of the variation in their values.

The data used are based on the analysis and processing of hydrogeological and hydrochemical measurements in the study area, which have been carried out in current and previous hydrogeological investigations in the study area [25,33–35].

Finally, a comparison is made of the results from the application of the SITE and SIVI methods with the results obtained from the investigation of groundwater vulnerability with the GALDIT method in the same area. The whole process of calculating GVI (GALDIT vulnerability index), SITE and SIVI values is presented in Tables 4–7.

Table 4. Calculation of GVI values.

	Well →	26	74	147	229	28	50	14	17	18	23
	G	Unconfined									
Groundwater occurrence (G)	W ₁	1	1	1	1	1	1	1	1	1	1
	R ₁	7.5	7.5	7.5	7.5	7.5	7.5	7.5	7.5	7.5	7.5
	W ₁ ×R ₁	7.5	7.5	7.5	7.5	7.5	7.5	7.5	7.5	7.5	7.5
	A (×10 ^{−5} m/s)	6.0	12.0	20.0	20.0	4.0	12.0	3.0	3.0	3.0	3.0
Aquifer hydraulic conductivity (A) *	A (m/day)	5.18	10.37	17.28	17.28	3.46	10.37	2.25	2.59	2.59	2.59
	W ₂	3	3	3	3	3	3	3	3	3	3
	R ₂ (rating)	5	7.5	7.5	7.5	2.5	7.5	2.5	2.5	2.5	2.5
	W ₂ ×R ₂	15.0	22.5	22.5	22.5	7.5	22.5	7.5	7.5	7.5	7.5
Height of groundwater level above sea level (L)—April 2023	L (m)	7.57	6.10	4.26	2.80	2.95	0.35	10.35	3.63	2.80	2.88
	W ₃	4	4	4	4	4	4	4	4	4	4
	R ₃	2.5	2.5	2.5	2.5	2.5	10	2.5	2.5	2.5	2.5
Height of groundwater level above sea level (L)—October 2023	W ₃ ×R ₃	10	10	10	10	10	40	10	10	10	10
	L (m)	5.66	2.65	3.49	2.23	2.48	−0.45	8.30	3.18	2.96	2.89
	W ₃	4	4	4	4	4	4	4	4	4	4
	R ₃	2.5	2.5	2.5	2.5	2.5	10	2.5	2.5	2.5	2.5
	W ₃ ×R ₃	10	10	10	10	10	40	10	10	10	10
	D (m)	7113	6443	4796	3730	4187	1965	5910	4327	3343	2433
Distance from the shore (D)	W ₄	4	4	4	4	4	4	4	4	4	4
	R ₄	5	5	7.5	7.5	7.5	10	5	7.5	7.5	10
	W ₄ ×R ₄	20	20	30	30	30	40	20	30	30	40
Impact of existing status of seawater intrusion (I)	I (Revelle)	0.84	3.57	1.79	1.98	0.82	1.57	0.45	1.16	0.40	0.78
	W ₅	1	1	1	1	1	1	1	1	1	1
	R ₅	2.5	10.0	7.5	7.5	2.5	7.5	2.5	5	2.5	2.5
	W ₅ ×R ₅	2.5	10	7.5	7.5	2.5	7.5	2.5	5	2.5	2.5
	T (m)	27	27	27	27	27	27	27	27	27	27
Thickness of the aquifer (T) (m)	W ₆	2	2	2	2	2	2	2	2	2	2
	R ₆	10	10	10	10	10	10	10	10	10	10
	W ₆ ×R ₆	20	20	20	20	20	20	20	20	20	20
GVI April 2023		5.0	6.0	6.5	6.5	5.2	9.2	4.5	5.3	5.2	5.8
GVI October 2023		5.0	6.0	6.5	6.5	5.2	9.2	4.5	5.3	5.2	5.8

Note: *: [24,36].

Table 5. Parameter values for the calculation of SITE and SIVI index values (April and October 2023) (valuation and characterization of values from [9,19]).

Cl (mg/L)	0–250 mg/L		≥ 250 mg/L		
S_{α} (km ²)	18.46		23.00		
S_t (km ²)		41.46			
$S \rightarrow$		0.555			
Cl (mg/L)	250–532.80/L		532.80–815.58 mg/L		
S_i (km ²)	16.478		6.522		
\overline{Cl}_n (mg/L)	391.40		674.20		
$S_i \times \overline{Cl}_n$ (km ²)	6449.489		4397.132		
$I \rightarrow$		471.592			
year	\overline{Cl}_n (\bar{f}) (mg/L)	$\frac{1}{n} \sum_{x=1}^n f(x)$ (2023) (mg/L)	\bar{f} (mg/L) (2021, 2022, 2023)	T_0 ↓	T ↓
2021 *	324.81				
2022 **	295.82	326.41	315.68	0.034	0.042
2023	326.41				
\overline{Cl}_{n-1} (mg/L) (2022 **)		\overline{Cl}_n (mg/L) (2023)		E ↓	
295.82		326.41		1.103	
K (m/s) ***	$0-8 \times 10^{-5}$ m/s		$>8 \times 10^{-5}$ m/s		
S_i (km ²)	9.76		13.24		
S_b (km ²)		13.24			
S_t (km ²)		23.00			
$C \rightarrow$		0.576			
h (m)	<1.0 m **** April 2023		<1.0 m **** October 2023		
S_c (km ²)	2.37		2.90		
S_t (km ²)		41.46			
$H \rightarrow$	0.057		0.070		
Distance from shoreline ****	S_d (km ²)	S_t (km ²)	D ↓		
>7 km	38.09	41.46	0.919		

Notes: *: [36], **: [37], ***: [24,25,38–40], ****: in combination with Figures 1 and 5.

Table 6. Calculation of SITE and SIVI index values (April 2023, October 2023) (valuation and characterization of values from [9,11]).

	Calculated Value	Assigned Value	Characterization
S	0.555	3	High
I	471.592	1	low
T	0.042	0	Very low
E	1.103	1	Moderate deterioration
A	Unconfined	3	High
C	0.576	3	High
H (April 2023)	0.057	0	Very low
H (October 2023)	0.070	0	Very Low
D	0.919	2	Very Far
SITE value \rightarrow		0.408	Moderate
SIVI Index \rightarrow		0.464 (April and October 2023)	Moderate

Table 7. Calculation of SIVI index values for the study area and for each monitoring well (April 2023 and October 2023).

			26	74	147	229	28	50	14	17	18	23
Cl [−]	July 2023	(mg/L)	63.83	585.09	407.79	460.98	257.09	815.58	99.29	390.06	99.29	85.10
Hydraulic conductivity		($\times 10^{-5}$ m/s)	6.0	12.0	20.0	20.0	4.0	12.0	3.0	3.0	3.0	3.0
Water table (h)	April 2023	(m)	7.57	6.10	4.26	2.80	2.95	0.35	10.35	3.63	2.80	2.88
	October 2023	(m)	5.66	2.65	3.49	2.23	2.48	−0.45	8.30	3.18	2.96	2.89
Distance from shoreline (d)		(m)	7113	6443	4796	3730	4187	1965	5910	4327	3343	2433
S		cv	−	0.555	0.555	0.555	0.555	0.555	−	0.555	−	−
		av	0	3	3	3	3	3	0	3	0	0
I		cv	−	471.592	471.592	471.592	471.592	471.592	−	471.592	−	−
		av	0	1	1	1	1	1	0	1	0	0
T		cv	0.042	0.042	0.042	0.042	0.042	0.042	0.042	0.042	0.042	0.042
		av	0	0	0	0	0	0	0	0	0	0
E		cv	1.103	1.103	1.103	1.103	1.11	1.103	1.103	1.103	1.103	1.103
		av	1	1	1	1	1	1	1	1	1	1
A		cv	UA	UA	UA	UA	UA	UA	UA	UA	UA	UA
		av	3	3	3	3	3	3	3	3	3	3
C		cv	−	0.576	0.576	0.576	−	0.576	−	−	−	−
		av	0	3	3	3	0	3	0	0	0	0
H	April 2023	cv	−	−	−	−	−	0.057	−	−	−	−
		av	0	0	0	0	0	0	0	0	0	0
	October 2023	cv	−	−	−	−	−	0.070	−	−	−	−
		av	0	0	0	0	0	1	0	0	0	0
D		cv	−	0.919	0.919	0.919	−	0.919	−	0.919	−	−
		av	0	2	2	2	0	2	0	2	0	0
SIVI Index (April 2023)			0.14	0.46	0.46	0.46	0.29	0.50	0.14	0.36	0.14	0.14
SIVI Index (October 2023)			0.14	0.46	0.46	0.46	0.29	0.50	0.14	0.36	0.14	0.14

Notes: cv/av: calculated value/assigned value, UA: unconfined aquifer.

Table 4 shows the procedure for calculating the GVI values.

Based on the results of the GALDIT method in the study area, a vulnerability map was designed for April and October 2023 (Figure 13). The map shows four (4) zones of groundwater vulnerability to seawater intrusion in the area. From the comparison of the distribution map of the GALDIT index values for both study periods with the distribution map of chloride concentration (Figure 5), a relative identification of the high vulnerability parts with the parts of moderate pollution from seawater intrusion and correspondingly with the parts with increased chloride concentration values is observed. This is an initial serious proof step to demonstrate the credibility of the effort to assess groundwater vulnerability in the study area from seawater intrusion using the GALDIT method. The identification of the part with high vulnerability that extend mainly south towards the coastline is established.

The following are important points regarding the process of calculating SITE and SIVI values (Table 5):

- Reference value (higher acceptable value) $V_r = 250$ mg/L (Ministerial Decision 1811/2011—Official Gazette 3322/B' 30 December 2011).
- The characterization of the S, I, T, E, A, C, H, D values is based on relative ranges of value variation as presented in corresponding tabulations of [9,19].
- The denominators of Equations (9) and (10) (Table 1) have the values 30 and 28, respectively, because these are the maximum values that the SITE and SIVI indices can take.
- Regarding the valuation of the aquifer under investigation, which is an unconfined aquifer [16], parameter (A) was evaluated with the assigned value of 3 (high vulnerability) (Tables 2 and 6).

- The area measurement of individual sections: [A] $\text{Cl}^- \geq 250 \text{ mg/L}$ (23.00 km²) (in red), [B] $\text{Cl}^- < 250 \text{ mg/L}$ (18.46 km²) (all remaining section) (Figure 14) was carried out after a similar demarcation of the sections based on the maps of Figures 1 and 5 (total area St: 41.46 km²).
- Based on the results from pumping tests in the study area [24] and in combination with Figure 14, it emerged that the value of $8 \times 10^{-5} \text{ m/s}$ can be characterized as the reference value for the C parameter.
- Based on the piezometric maps of Figure 4 and in combination with Figures 5 and 14, height of groundwater level parameter (L) was calculated. Based on Equation (7), as presented in Table 2 and according to [9], the value of 1.0 m is taken as the (L) reference value for April and October 2023.

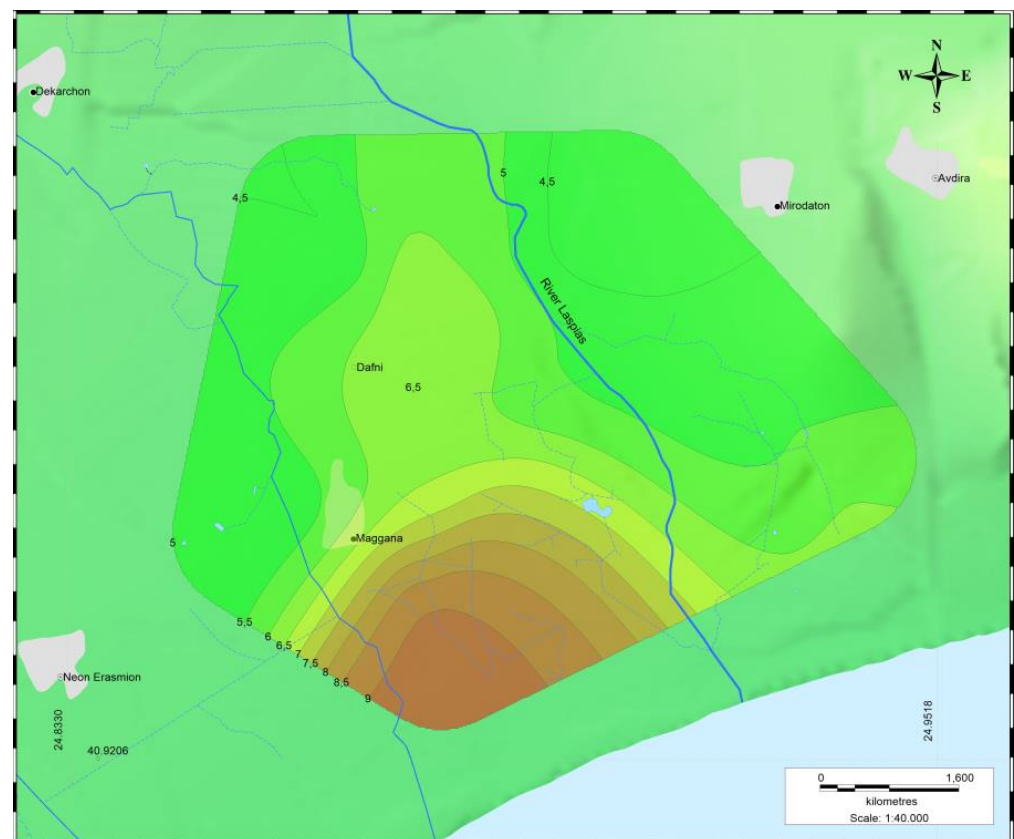


Figure 13. GALDIT vulnerability index (GVI) values distribution map.

In Table 6, it can be seen that the final values of the SITE and SIVI indices for the entire study area amount to 0.408 (SITE) and 0.464 (SIVI) (for both April and October 2023), with consequent characterization of the vulnerability of the study aquifer to seawater intrusion as Moderate [19].

Finally, a comparison is made of the results from the application of the SITE and SIVI methods with the results obtained from the investigation of groundwater vulnerability with the GALDIT method in the same area.

Table 7 presents the results from the calculation of SIVI index values for the study area and for each monitoring well (April and October 2023) based on Equation (10) (Table 2). Then follows the presentation of a distribution map of SIVI vulnerability index values designed taking into account SIVI index values for each well for the months of April and October 2023 (Figure 15). More specifically, the SIVI index values vary from 0.14 to 0.50 for both April and October 2023. The highest values of the index appear in the south of the study area.

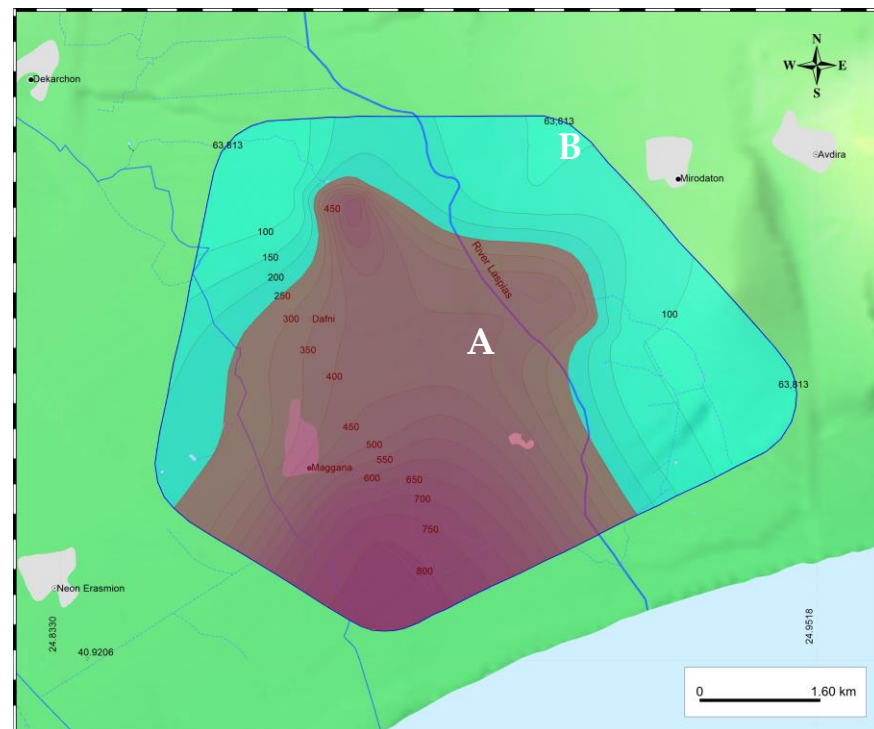


Figure 14. Demarcation of sections: (A) $\text{Cl}^- \geq 250 \text{ mg/L}$ (red color), (B) $\text{Cl}^- < 250 \text{ mg/L}$ (the entire remaining section).

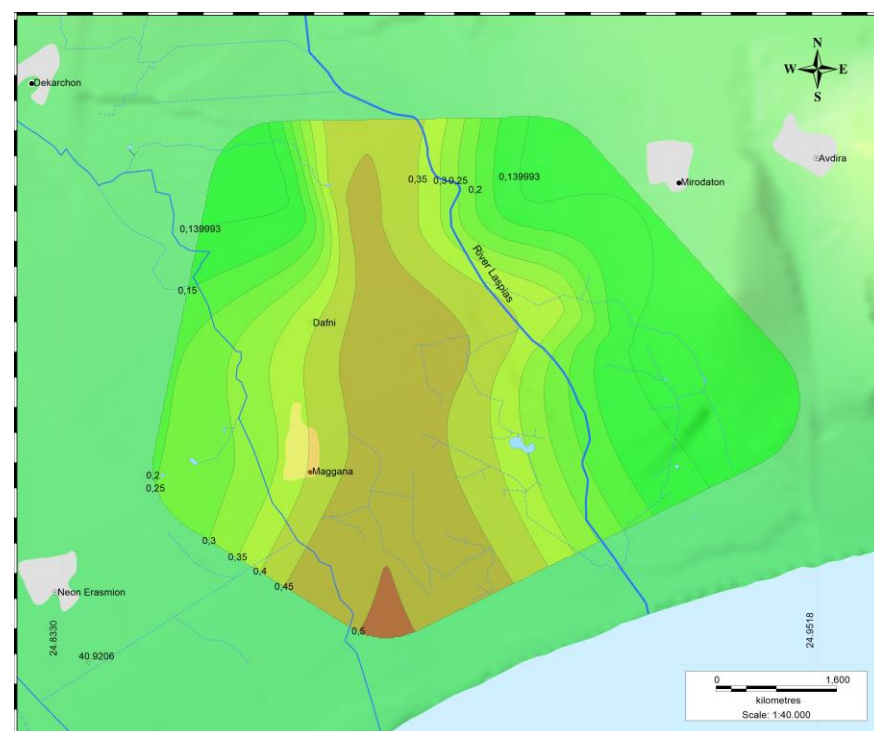


Figure 15. SIVI vulnerability index values distribution map.

From the analysis of the SIVI vulnerability index distribution map, it was found that the variation in the SIVI index values is the same for both calculation periods. From the comparison of the distribution map of the SIVI index for both study periods with the distribution maps of the chloride (Cl^-) concentration values and the electrical conductivity

(EC) values, as well as the distribution maps of the GALDIT vulnerability index, the following can be concluded:

- There is a relative identification of the parts of greater vulnerability with the parts of moderate pollution from seawater intrusion and with the parts with increased chloride concentration values. This is a strong piece of evidence in highlighting the reliability of the effort to assess groundwater vulnerability of the study area to seawater intrusion with the SITE and SIVI methods.
- It is found that, in April and October 2023, the values of the SIVI index increased towards the southeast part, with a maximum value of 0.50, while the values decreased towards the east part and the north NW part, with a minimum value of 0.14.
- A relative matching in the southeastern part of the study area is found, between the SIVI vulnerability index (Figure 15) and chloride (Cl^-) concentration values, with a maximum value of 815.5 (Figure 5), and electrical conductivity (EC) values, with a maximum value of 3770 $\mu\text{S}/\text{cm}$ (Figure 6), as well as the GALDIT vulnerability index (GVI) values, with a maximum value of 9.2 (Figure 13).

4. Conclusions

This paper describes the investigation of coastal groundwater vulnerability to seawater intrusion in the coastal area of Laspias River, NE Greece, using GALDIT, SITE and SIVI methods, in the context of groundwater management in the area. Using the geological, hydrological and hydrogeological data from the relevant measurements of the area for the time periods of April and October 2023, the unconfined aquifer was mapped with the distinction in vulnerability zones.

The application of the methods and the calculation of the values of each method was achieved by relative tabulation of the process and the subsequent design of vulnerability maps. During GALDIT method application, specific characteristics of the aquifer of the study area were involved in the calculation related to hydrogeological, hydrochemical and spatial data (type of aquifer, hydraulic conductivity, distance from coastline, thickness of aquifer, altitude of groundwater level, Revelle values). The SIVI and SITE method procedures took into account data similar to the GALDIT method (aquifer type, hydraulic conductivity, distance from coastline, altitude of groundwater level), as well as some additional data related to the extent of the affected area by seawater intrusion, its seasonality and evolution of seawater intrusion based on the concentrations of chloride ions in groundwater at various sites in the aquifer throughout space and time.

All three methods, despite the advantages and disadvantages of each method, as described especially in the introduction of this paper, come to the conclusion that high vulnerability values extend mainly south towards the coastline of the study area corresponding to the parts with increased values of chloride concentration and electrical conductivity, thus enhancing the reliability of the research procedure of assessing groundwater vulnerability to seawater intrusion in the study area.

It would be very interesting to assess and evaluate the vulnerability of the system over the last decade or more. The process is proposed to include the application of GALDIT, SITE and SIVI methods with as much available hydrological and hydrogeological data and information as can be collected. The results would be very useful in conducting the most reliable hydrogeological assessment of the hydrogeological regime of the system and can significantly contribute to the planning of further research and activities in the context of the rational utilization and management of the groundwater potential at the eastern Delta of the Nestos River.

Author Contributions: Conceptualization, methodology, C.P., I.G. and F.-K.P.; writing—original draft preparation, review and editing, C.P., I.G., D.K., P.A., A.K. and F.-K.P.; validation, supervision, I.G. and F.-K.P. All authors have read and agreed to the published version of the manuscript.

Funding: This research received no external funding.

Data Availability Statement: The relevant data can be found in this article.

Acknowledgments: The results of this paper are part of the research of the Doctoral Dissertation of Christina Pliaka, MSc civil engineer, Department of Civil Engineering, School of Engineering, Democritus University of Thrace, Greece.

Conflicts of Interest: The authors declare no conflicts of interest.

References

1. Parizi, E.; Hosseinia, S.M.; Ataie-Ashtianib, B.; Simmons, C.T. Vulnerability mapping of coastal aquifers to seawater intrusion: Review, development and application. *J. Hydrol.* **2019**, *57*, 555–573. [\[CrossRef\]](#)
2. Alongi, D.M. *Coastal Ecosystem Processes*; CRC Press: Boca Raton, FL, USA, 1999.
3. Tan, W.J.; Yang, C.F.; Châteauc, P.A.; Leed, M.T.; Chang, Y.C. Integrated coastal-zone management for sustainable tourism using a decision support system based on system dynamics: A case study of Cijin, Kaohsiung, Taiwan. *Ocean Coast. Manag.* **2018**, *153*, 131–139. [\[CrossRef\]](#)
4. Klassen, J.; Allen, D.M. Assessing the Risk of Saltwater Intrusion in Coastal Aquifers. *J. Hydrol.* **2017**, *551*, 730–745. [\[CrossRef\]](#)
5. Kallioras, A.; Pliakas, F.; Skias, S.; Gkioungkis, I. Groundwater vulnerability assessment at SW Rhodope aquifer system in NE Greece. In *Advances in the Research of Aquatic Environment*; Lambrakis, N., Stournaras, G., Katsanou, K., Eds.; Springer: Berlin/Heidelberg, Germany, 2011; pp. 351–358. [\[CrossRef\]](#)
6. Kura, N.U.; Ramli, M.F.; Ibrahim, S.; Sulaiman, W.N.A.; Aris, A.Z.; Tanko, A.I.; Zaudi, M.A. Assessment of groundwater vulnerability to anthropogenic pollution and seawater intrusion in a small tropical island using index-based methods. *Environ. Sci. Pollut. Res.* **2014**, *22*, 1512–1533. [\[CrossRef\]](#) [\[PubMed\]](#)
7. Luoma, S.; Okkonen, J.; Korkka-Niemi, K. Comparison of the AVI, modified SINTACS and GALDIT vulnerability methods under future climate-change scenarios for a shallow low-lying coastal aquifer in southern Finland. *Hydrogeol. J.* **2017**, *25*, 203–222. [\[CrossRef\]](#)
8. Kazakis, N.; Spiliotis, M.; Voudouris, K.; Pliakas, F.-K.; Papadopoulos, B. A fuzzy multicriteria categorization of the GALDIT method to assess seawater intrusion vulnerability of coastal aquifers. *Sci. Total Environ.* **2018**, *621*, 524–534. [\[CrossRef\]](#) [\[PubMed\]](#)
9. Zeynolabedin, A.; Ghiass, R. The SIVI index: A comprehensive approach for investigating seawater intrusion vulnerability for island and coastal aquifers. *Environ. Earth Sci.* **2019**, *78*, 666. [\[CrossRef\]](#)
10. Lobo-Ferreira, J.P.; Chachadi, A.G.; Diamantino, C.; Henriques, M.J. Assessing aquifer vulnerability to seawater intrusion using GALDIT method: Part 1—Application to the Portuguese Aquifer of Monte Gordo. In *Proceedings of the 4th InterCeltic Colloquium on Hydrology and Management of Water “Water in Celtic Countries: Quantity, Quality and Climate Variability”*, Guimarães, Portugal, 11–13 July 2005; Ferreira, J.P.L., Vieira, M.P., Eds.; 2005; pp. 161–171.
11. Pedreira, R.; Kallioras, A.; Pliakas, F.; Gkioungkis, I.; Schuth, C. Groundwater vulnerability assessment of a coastal aquifer system at River Nestos eastern Delta, NE Greece. *Environ. Earth Sci.* **2015**, *73*, 6387–6415. [\[CrossRef\]](#)
12. Recinos, N.; Kallioras, A.; Pliakas, F.; Schuth, C. Application of GALDIT index to assess the intrinsic vulnerability to seawater intrusion of coastal granular aquifers. *Environ. Earth Sci.* **2015**, *73*, 1017–1032. [\[CrossRef\]](#)
13. Najib, S.; Fadili, A.; Mehdi, K.; Riss, J.; Makan, A.; Guessir, H. Salinization process and coastal groundwater quality in Chaouia Morocco. *J. Afr. Earth Sci.* **2016**, *115*, 17–31. [\[CrossRef\]](#)
14. Amarni, N.; Fernane, L.; Naili, M.; Lounas, R.; Belkessa, R. Mapping of the vulnerability to marine intrusion “in coastal Cherchell aquifer, Central Algeria” using the GALDIT method. *Groundw. Sustain. Dev.* **2020**, *11*, 100481. [\[CrossRef\]](#)
15. Boufekane, A.D.; Maizi, E.; Madene, G.; Busico, A.; Zghibi, A. Hybridization of GALDIT method to assess actual and future coastal vulnerability to seawater intrusion. *J. Environ. Manag.* **2022**, *318*, 115580. [\[CrossRef\]](#) [\[PubMed\]](#)
16. Nadiri, A.A.; Bordbar, M.; Nikoo, M.R.; Silabi, L.S.S.; Senapathi, V.; Xiao, Y. Assessing vulnerability of coastal aquifer to seawater intrusion using Convolutional Neural Network. *Mar. Pollut. Bull.* **2023**, *197*, 115669. [\[CrossRef\]](#) [\[PubMed\]](#)
17. Chronidou, D.; Tziritis, E.; Panagopoulos, A.; Oikonomou, E.K.; Loukas, A. A Modified GALDIT Method to Assess Groundwater Vulnerability to Salinization—Application to Rhodope Coastal Aquifer (North Greece). *Water* **2022**, *14*, 3689. [\[CrossRef\]](#)
18. Setiawan, I.; Morgan, L.K.; Doscher, C. Mapping the vulnerability of groundwater to saltwater intrusion from estuarine rivers under sea level rise. *J. Hydrol.* **2024**, *628*, 130461. [\[CrossRef\]](#)
19. Ballesteros, B.J.; Morell, I.; García-Menéndez, O.; Renau-Pruñonosa, A. A standardized index for assessing seawater intrusion in coastal aquifers: The SITE index. *Water Resour. Manag.* **2016**, *30*, 4513–4527. [\[CrossRef\]](#)
20. Mavriou, Z.; Kazakis, N.; Pliakas, F.-K. Assessment of groundwater vulnerability in the north aquifer area of Rhodes Island using the GALDIT method and GIS. *Environ. J.* **2019**, *6*, 56. [\[CrossRef\]](#)
21. Chachadi, A.G.; Raikar, P.S.; Lobo Ferreira, J.P.; Oliveira, M.M. *GIS and Mathematical Modelling for the Assessment of Groundwater Vulnerability to Pollution: Application to an Indian Case Study Area in Goa*; Laboratório Nacional de Engenharia Civil. Lisboa Laboratório: Lisboa, Portugal, 2001.
22. Chachadi, A.G.; Lobo-Ferreira, J.P. Sea water intrusion vulnerability mapping of aquifers using GALDIT method. *Coastin A Coast. Policy Res. Newsl.* **2001**, *4*, 7–9.
23. Chachadi, A.G.; Lobo-Ferreira, J.P. Assessing aquifer vulnerability to sea water intrusion using GALDIT method: Part 2-GALDIT Indicators Description. In *Proceedings of the Fourth Inter-Celtic Colloquium on Hydrology and Management of Water Resources*, Guimarães, Portugal, 11–14 July 2005.

24. Gkiougkis, I. Investigation of Seawater Intrusion in Coastal Aquifers in Deltaic Environment. The Case of Nestos River Delta. Ph.D. Thesis, Department of Civil Engineering, Democritus University of Thrace, Xanthi, Greece, 2018. (In Greek).
25. Gkiougkis, I.; Pouliaris, C.; Pliakas, F.-K.; Diamantis, I.; Kallioras, A. Conceptual and Mathematical Modeling of a Coastal Aquifer in Eastern Delta of R. Nestos (N. Greece). *Hydrol. J.* **2021**, *8*, 23. [[CrossRef](#)]
26. Sakkas, I.; Diamantis, I.; Pliakas, F. *Groundwater Artificial Recharge Study of Xanthi—Rhodopi Aquifers (in Thrace, Greece)*. Greek Ministry of Agriculture Research Project, Final Report; Sections of Geotechnical Engineering and Hydraulics of the Civil Engineering Department of Democritus University of Thrace: Xanthi, Greece, 1998. (In Greek)
27. Kallergis, G. *Applied—Environmental Hydrogeology*; TCG: Athens, Greece, 2000; Volume B, 345p. (In Greek)
28. Ayers, R.S. Quality of water for irrigation. In Proceedings of the Irrigation and Drainage Division, Specialty Conference, ASCE, Logan, Utah, 13–15 August 1975; pp. 24–56.
29. Richards, L.A. *Diagnosis and Improvement of Saline Alkali Soils*; Handbook No. 60; USDA: Washington, DC, USA, 1954; 160p.
30. Wilcox, L.V. *Classification and Use of Irrigation Waters*; Agric. Circ.: Washington, DC, USA, 1955.
31. Revelle, R. Criteria for recognition of sea water in ground waters. *Trans. Amer. Geophys. Union* **1941**, *22*, 593–597.
32. Soulios, G. *Hydrogeology*; University Studio Press: Thessaloniki, Greece, 2006; Volume D. (In Greek)
33. Gkiougkis, I.; Tzeveleakis, T.; Pliakas, F.; Diamantis, I.; Pechtelidis, A. Geophysical research of groundwater degradation at the eastern Nestos River Delta, NE Greece. *Adv. Res. Aquat. Environ. Environ. Earth Sci.* **2011**, *1*, 259–266.
34. Gkiougkis, I.; Kallioras, A.; Pliakas, F.; Pechtelidis, A.; Diamantis, V.; Diamantis, I.; Ziogas, A.; Dafnis, I. Assessment of soil salinization at the eastern Nestos River Delta, N.E. Greece. *Cateba* **2015**, *128*, 238–251. [[CrossRef](#)]
35. Lymperiadou, G.; Gkiougkis, I.; Karasogiannidis, D.; Pliakas, F.-K. Research for the updated conceptual model of a coastal aquifer in River Nestos Eastern Delta. In Proceedings of the 12th International Hydrogeological Conference, Nicosia (Lefkosia), Cyprus, 20–22 March 2022; pp. 336–344.
36. Gkiougkis, I.; Adamidis, A.; Empliouk, I.; Karasogiannidis, D.; Pliaka, C.; Tzeveleakis, T.; Pliakas, F.-K. Research for The Conceptual Model Development of River Lissos Coastal Aquifer System, NE Greece. In Proceedings of the 16th International Congress of the Geological Society of Greece, Patras, Greece, 17–19 October 2022; pp. 450–451.
37. Pliakas, F.-K.; Gkiougkis, I.; Pliaka, C.; Karasogiannidis, D.; Adamidis, A.; Empliouk, I. *Project Eye4water (MIS 5047246): Strengthening the Water Management Practices (in EMT-R) through the Development of Innovative ICT Methodologies and Improvement of Research Infrastructures*; Deliverable 2.3, 1. Technical Report of Groundwater Quality Status (19-5-2023); Eye4water: Xanthi, Greece, 2023.
38. Kallergis, G. *Applied—Environmental Hydrogeology*; TCG: Athens, Greece, 1999; Volume A, 345p. (In Greek)
39. Todd, D.K.; Mays, L.W. *Groundwater Hydrology*, 3rd ed.; John Wiley and Sons Inc.: New York, NY, USA, 2005.
40. Domenico, P.A.; Schwartz, W. *Physical and Chemical Hydrogeology*; Wiley: New York, NY, USA, 1998.

Disclaimer/Publisher’s Note: The statements, opinions and data contained in all publications are solely those of the individual author(s) and contributor(s) and not of MDPI and/or the editor(s). MDPI and/or the editor(s) disclaim responsibility for any injury to people or property resulting from any ideas, methods, instructions or products referred to in the content.